JOURNAL OF SOLID STATE CHEMISTRY **122,** 231–238 (1996)
ARTICLE NO. 0106

Synthesis and Characterization of Mixed Fe–Cr Oxide Pillared α-Zirconium Phosphate Materials

F. J. Perez-Reina, P. Olivera-Pastor, E. Rodriguez-Castellon, and A. Jimenez-Lopez

Departamento de Química Inorgánica, Cristalograffía y Mineralogía, Facultad de Ciencias, Universidad de Málaga, 29071 Málaga, Spain

and

J. L. G. Fierro

Instituto de Catálisis y Petroleoquímica, C.S.I.C., Campus Universidad Autónoma, 28049 Madrid, Spain

Received August 7, 1995; in revised form November 22, 1995; accepted December 14, 1995

Mixed Fe/Cr hydroxyacetate oligomers ranging in composition from 90/10 to 10/90 have been prepared by mixing Fe^{3+} and Cr^{3+} nitrate solutions and then adding *n*-propylammonium acetate up to an acetate/Cr^{3+} ratio of 2.8 and pH 4. The oligomers were intercalated into colloidal α-zirconium phosphate or precipitated with excess *n*-propylamine. The precipitates are all amorphous and show differential thermal behavior in comparison with the intercalates. Upon calcination in air, the precipitates become crystalline, showing the characteristic XRD peaks of mixed Fe/Cr oxides. These mixed oxides present unusually high BET surface areas (up to 276 $m^2 \cdot g^{-1}$), especially those with low Fe/Cr ratios. The intercalates are poorly crystalline or amorphous at room temperature and upon calcination at 400°C in air or under N_2, which indicates that there is no oxide segregation from the interlayers. From these results it is suggested that mixed Fe/Cr oxides are cross-linked to the phosphate layer, forming a pillared structure. Significantly, the mixed oxides segregated from the phosphate surface at 1000°C present XRD patterns identical to the mixed oxides obtained from the precipitates with the same Fe/Cr ratios. The pillared materials show high BET surface areas, from 200 to 306 m^2/g, and narrow pore size distributions with pore radius ranging from 8.5 to 13.8 Å. XPS analysis reveals a higher affinity of the phosphate surface for Cr^{3+} at high Fe/Cr ratios from 70/30 to 90/10. In these samples the partial oxidation of Cr(III) to Cr(VI) was observed in the XPS spectra, in spite of the materials being calcined under N_2. © 1996 Academic Press, Inc.

INTRODUCTION

There is an increasing interest in finding new methods for producing porous solids. Pillaring of layered compounds by insertion of inorganic oligomer species is an important way to prepare micro- or mesoporous solids with high surface area and acidity to be used in catalytic reactions, where high activities and selectivities are required (1, 2).

Metal (IV) layered phosphates are appropriate matrices in which to intercalate inorganic oligomers by ion exchange which lead to very different porous solids, useful as catalysts, ion exchangers and absorbents (3).

The number of inorganic cations capable to form oligomers in optimum conditions to be inserted into the layered phosphate is limited, but the use of mixed oligomers opens many possibilities. We have recently reported the preparation of mixed alumina–chromia pillared α-zirconium phosphates, with much higher specific surface areas and porosities than their homologous alumina and chromia pillared materials (4). In a similar way, Fe/Al oxide pillared clays exhibit enhanced acidity with respect to the alumina pillared clays (5).

Given that Fe^{3+} and Cr^{+3} oxides are isomorphous and miscible in all ranges of composition, it would be very interesting to investigate the properties of Fe/Cr oxide pillared materials to be applied to heterogeneous catalysis, taking into account the important applications of these mixed oxides in the water-gas shift reaction (6), dehydrogenation of hydrocarbons (7), oxidative dehydrogenation of butenes to butadienes (8), etc.

In the present work, we report the preparation and characterization of mixed Fe–Cr oxide pillared α-zirconium phosphate, using chemical and thermal analysis, spectroscopic techniques including XRD, IR, diffuse reflectance, and X-ray photoelectron spectroscopy (XPS), and N_2 adsorption.

EXPERIMENTAL

Materials

The initial material, α-zirconium phosphate (α-ZrP), was synthesized by the sol–gel method (9). This α-ZrP was then suspended in deionized water and colloidized by neu-

0022-4596/96 $18.00
Copyright © 1996 by Academic Press, Inc.
All rights of reproduction in any form reserved.

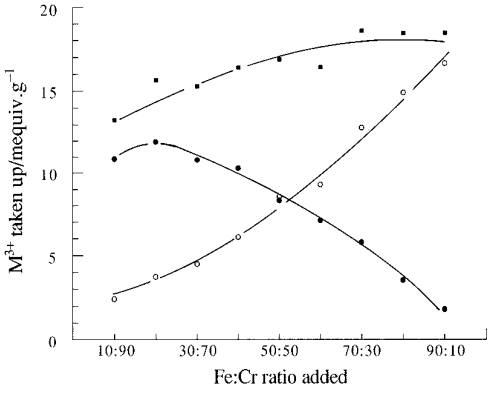

FIG. 1. Uptake of iron and chromium from mixed Fe/Cr solutions by colloidal α-zirconium phosphate: (○) Fe, (●) Cr, (■) Fe + Cr.

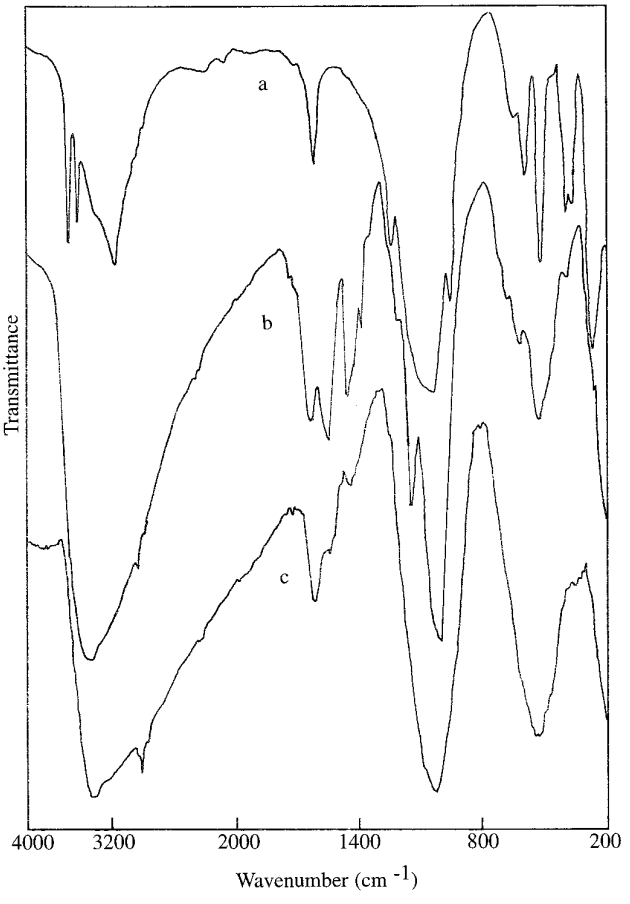

FIG. 2. Infrared spectra of (a) α-ZrP, (b) precursor Fe/Cr 50/50 at 25°C, and (c) pillared Fe/Cr 50/50 at 400°C.

tralization with 0.1 mol dm^{-3} *n*-propylamine solution up to 60% of the cation exchange capacity. Any flocculated product was discarded.

The mixed Fe–Cr pillaring solutions were prepared by dissolving $Fe(NO_3)_3 \cdot 9H_2O$ and $Cr(NO_3)_3 \cdot 9H_2O$ together in water. *n*-Propylammonium acetate and 0.1 mol dm^{-3} *n*-propylamine were then added to obtain a pH 4.4–4.5 and an $OAc^- : Cr^{+3}$ molar ratio of 2.8.

The mixed Fe–Cr pillaring solutions, with a total $[Fe^{3+}] + [Cr^{+3}]$ equal to 10 times the cationic exchange capacity of the α-ZrP (6.64 meq g^{-1}), were placed in contact with a colloidal suspension containing 1 g of α-ZrP and refluxed for 48 hr.

After reaction, the solids were separated by centrifugation, washed with deionized water up to a conductivity of washing water <50 μS, and air-dried.

Measurements

Chromium was determined colorimetrically using the chromate method ($\lambda = 372$ nm) and iron was analyzed by atomic absorption spectroscopy after treatment of samples with $NaOH/H_2O_2$. XRD of cast films was recorded on a Siemens D501 diffractometer (Cu$K\alpha$ radiation). TG and DTA analyses were carried out on a Rigaku Thermoflex instrument (calcined Al_2O_3 as reference and 10 K min^{-1}

TABLE 1
Chemical Composition and Empirical Formulations of Mixed Oligomeric Fe–Cr α-Zirconium Phosphate Intercalates

Fe/Cr ratio added	Fe/Cr ratio incorporated	Ac^-/Cr^{3+} ratio incorporated	Empirical Formulation
10/90	0.22	0.47	$Zr[Cr_{2.70}Fe_{0.60}(Ac)_{1.27}(OH)_{6.63}]\ (PO_4)_2 \cdot\ 6.4H_2O$
20/80	0.31	0.42	$Zr[Cr_{3.53}Fe_{1.10}(Ac)_{1.47}(OH)_{10.42}]\ (PO_4)_2 \cdot\ 5.4H_2O$
30/70	0.41	0.46	$Zr[Cr_{3.33}Fe_{1.38}(Ac)_{1.52}(OH)_{10.61}]\ (PO_4)_2 \cdot\ 6.9H_2O$
40/60	0.59	0.43	$Zr[Cr_{3.21}Fe_{1.90}(Ac)_{1.39}(OH)_{11.94}]\ (PO_4)_2 \cdot\ 5.2H_2O$
50/50	1.03	0.44	$Zr[Cr_{3.46}Fe_{3.56}(Ac)_{1.53}(OH)_{17.53}]\ (PO_4)_2 \cdot 11.2H_2O$
60/40	1.30	0.43	$Zr[Cr_{1.97}Fe_{2.56}(Ac)_{0.85}(OH)_{10.74}]\ (PO_4)_2 \cdot\ 3.9H_2O$
70/30	2.22	0.46	$Zr[Cr_{2.53}Fe_{5.61}(Ac)_{1.17}(OH)_{21.25}]\ (PO_4)_2 \cdot\ 8.7H_2O$
80/20	4.23	0.48	$Zr[Cr_{1.32}Fe_{5.58}(Ac)_{0.64}(OH)_{18.06}]\ (PO_4)_2 \cdot\ 6.5H_2O$
90/10	9.24	0.62	$Zr[Cr_{0.61}Fe_{5.64}(Ac)_{0.38}(OH)_{16.37}]\ (PO_4)_2 \cdot\ 4.9H_2O$

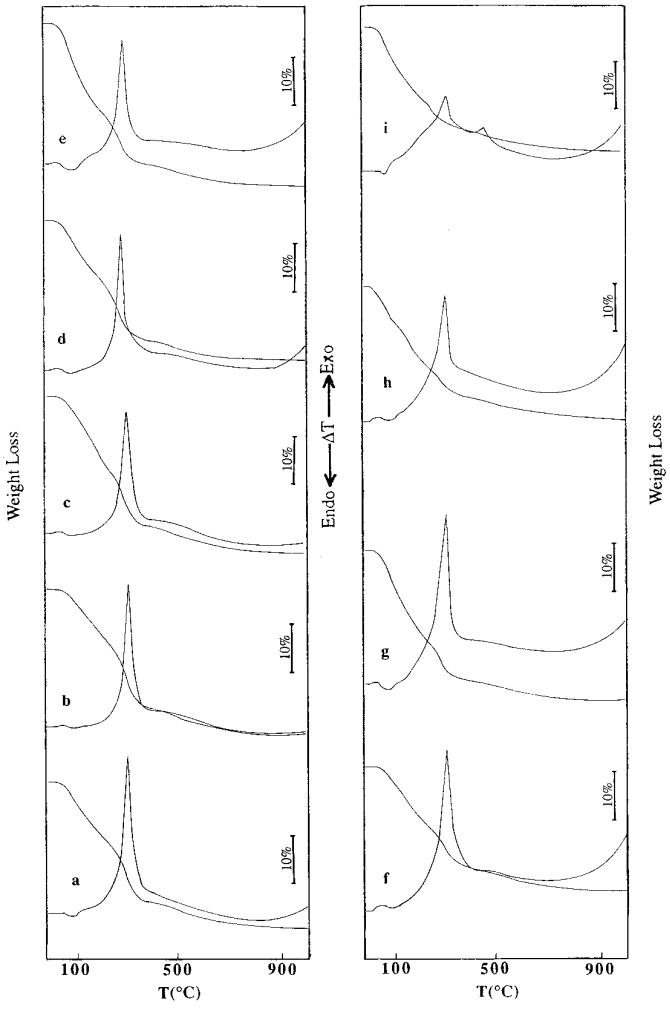

FIG. 3. Thermal analysis of mixed intercalates at Fe/Cr ratios of (a) 10/90, (b) 20/80, (c) 30/70, (d) 40/60, (e) 50/50, (f) 60/40, (g) 70/30, (h) 80/20, (i) 90/10.

heating rate). Electronic spectra (diffuse reflectance UV–VIS-near IR) were registered on a Shimadzu MPC 3100 spectrophotometer, and the IR spectra were obtained with a Perkin–Elmer 883 spectrometer. SEM photomicrographs of the samples were obtained using a JEOL SM 840. The XPS spectra were recorded with a Fison ESCALAB 200R spectrometer equipped with a Mg$K\alpha$ X-ray excitation source ($h\nu$ = 1253.6 eV) and hemispherical electron analyzer. The residual pressure in the ion-pumped chamber was maintained below 10^{-9} Torr during data acquisition. The binding energies (BE) were determined with ±0.2 eV accuracy and by charge referencing with the adventitious C 1*s* peak at 284.9 eV.

Asorption–desorption isotherms were determined on a conventional volumetric apparatus at 77 K, degassing at 473 K and 10^{-4} Torr (overnight).

RESULTS AND DISCUSSION

The individual and overall uptake curves of Cr^{3+} and Fe^{3+} by colloidal α-ZrP are shown in Fig. 1. The intercalation of mixed oligomers formed by hydrolysis causes the total amount of Cr^{3+} and Fe^{3+} taken up to exceed more by than twice the theoretical exchange capacity of the phosphate, and it slightly increases with the Fe/Cr ratio, probably due to that Fe^{3+} hydrolyzes in greater extent than Cr^{3+} (10). Table 1 lists the chemical compositions of the different intercalates obtained. Interestingly, the Fe/Cr ratios remain practically unchanged upon intercalation except for the sample with the lowest Fe^{3+} content. This would indicate that mixed oligomers are first formed in solution, according to the existent proportion of Cr^{3+} and Fe^{3+}, and then are intercalated into the phosphate with no modification in their composition.

Acetate is also incorporated into the mixed oligomers as a bidentade ligand, demonstrated by chemical analysis (Table 1), infrared spectroscopy ($\nu_{as}COO^-$ at 1550 cm^{-1}, $\nu_{sym}COO^-$ at 1450 cm^{-1}) (11) (Fig. 2), and thermal analysis. The acetate/Cr^{3+} ratio of the intercalated oligomers is almost constant in all ranges of composition, indicating that the acetate ligand is preferentially associated to Cr^{3+} ions. Although mixed Fe^{3+}/Cr^{3+} oxides are usually synthesized, in all range of composition, from basic mixed solutions (12, 13), our results reveal that acetate solutions of Fe^{3+} and Cr^{3+} can be also used to obtain mixed oxides.

DTA-TG curves of the intercalates (Fig. 3) show weight loss in three stages corresponding to removal of hydration water (100–160°C), combustion of acetate (160–350°C), and dehydroxylation (350–700°C). Only the 90/10 sample exhibits a small exothermic effect at 420°C. This effect has been also observed in thermal studies of amorphous chromia and mixed Fe/Cr oxides and related with the pres-

TABLE 2

XRD Reflection Data for Mixed Fe/Cr Oxide Pillared Materials, Synthetic Mixed Fe/Cr Oxides, and Reference Compounds

	d-spacing/Å						
α-Fe_2O_3[a]		3.684	2.700	2.519	2.207	1.841	1.694
α-Cr_2O_3[b]		3.631	2.665	2.479	2.175	1.816	1.672
Pillared Fe/Cr (1000°C):							
10/90	4.129	3.642	2.670	2.489	—	—	—
50/50	4.129	3.666	2.686	2.506	2.189	1.831	1.683
90/10	4.129	3.678	2.695	2.515	2.203	1.841	1.692
Mixed oxides Fe/Cr (1000°C):							
10/90		3.636	2.667	2.484	2.179	1.819	1.675
50/50		3.660	2.680	2.506	2.195	1.832	1.684
90/10		3.672	2.692	2.514	2.201	1.839	1.690

[a] CPDS File 33 664 (synthetic haematite).
[b] CPDS File 38 1479 (synthetic eskolaite).

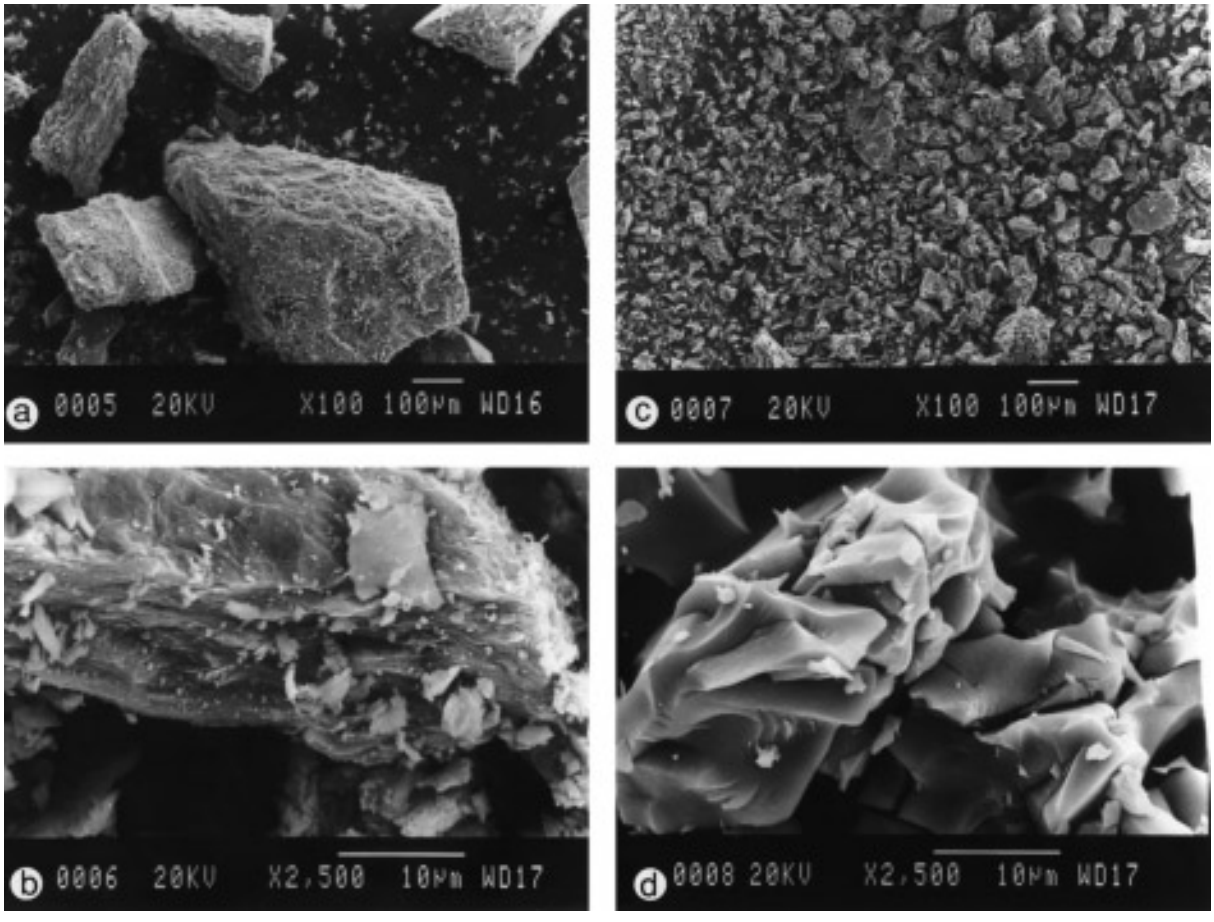

FIG. 4. SEM micrographs of Fe/Cr 50/50 pillared material (a, b) and Fe/Cr 50/50 precipitate (c, d). Magnification: 100 (a, c), 2500 (b, d).

ence of Cr(VI) oxide formed upon calcination, which is reduced to chromia at high temperature (13, 14).

XRD patterns show the trend of mixed intercalates to amorphize with increasing Fe^{3+} content. Materials with Fe/Cr ratios greater than 40/60 area amorphous, perhaps due to the existence of mixed oligomers with different sizes and charges. Samples with ratios of 10/90, 20/80, and 30/70 present very broad peaks, corresponding to basal spacings of 32.8, 25.1, and 21.6 Å, respectively. Upon thermal treatment at $T > 100$°C these materials also become amorphous.

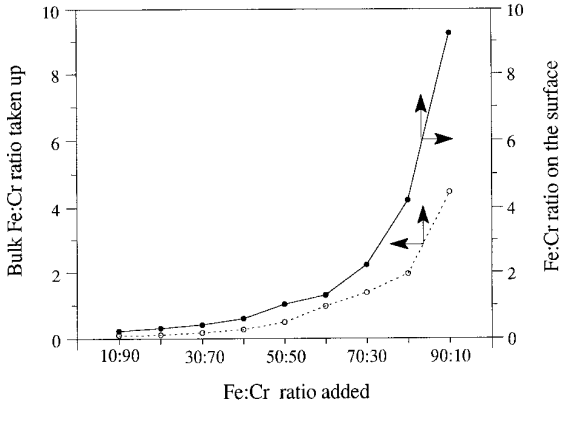

FIG. 5. Variation of bulk and surface Fe/Cr ratios with the Fe/Cr ratios added: (—) from chemical analysis, (---) from XPS.

For comparison, three mixed Fe/Cr acetohydroxide precipitates, with nominal ratios of 10/90, 50/50, and 90/10, have been prepared from the mixed oligomeric solutions. The precipitates are amorphous at room temperature and after calcination at 400°C under N_2, but they become crystalline after calcination in air at 400°C, showing broad XRD reflection lines characteristic of mixed Fe/Cr oxides (13) (Table 2).

The intercalated materials are amorphous after calcinination at 400°C in air or N_2, indicating that there is no segregation of oxide at this temperature. Calcination at 1000°C leads to a mixture of ZrP_2O_7 and a solid solution of mixed Fe/Cr oxides (Table 2). Significantly, the mixed oxides, formed from intercalated materials calcined at 1000°C, present the same XRD patterns than those of mixed oxides with identical Fe/Cr ratios, obtained by calcination of the precip-

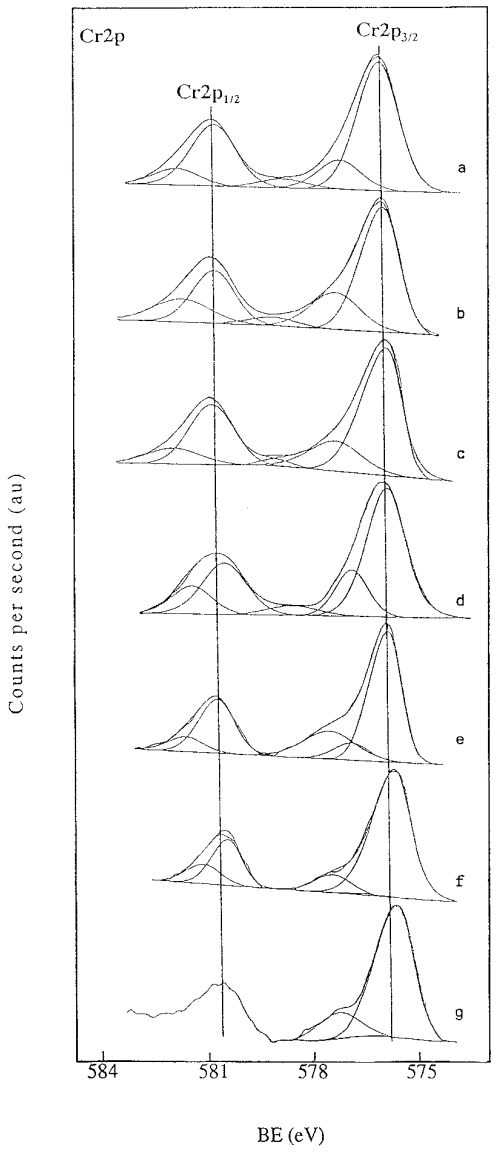

FIG. 6. XPS of mixed Fe/Cr oxide α-ZrP pillared materials: (a) 10/90, (b) 30/70, (c) 50/50, (d) 60/40, (e) 70/30, (f) 80/20, (g) 90/10.

itates at 1000°C. From the above results we infer that mixed Fe/Cr oxide pillared materials are obtained by calcination of the intercalates at 400°C, and that no superficial precipitation of hydroxides took place.

The morphology of mixed oxide pillared materials differs markedly from that of the corresponding mixed oxide (Fig. 4). The SEM micrographs of pillared materials show a clear habit of layered structure while those of the mixed oxides show a granulous aspect.

XPS Analysis

The near surface composition of the pillared materials has been determined by XPS analysis. Bulk and surface

TABLE 3

Binding Energies (eV) and Atomic P/Zr Ratio on the Surface (from XPS) of Mixed Fe/Cr Oxide Pillared α-Ziconium Phosphates

Sample	Zr $3d_{5/2}$	P $2p$	Cr $2p_{3/2}$	Fe $2p_{3/2}$	P/Zr
Fe/Cr 10 : 90	182.5	133.1	576.6	711.1	2.01
Fe/Cr 20 : 80	182.6	133.1	576.6	711.0	2.06
Fe/Cr 30 : 70	182.5	133.0	576.5	710.9	2.04
Fe/Cr 40 : 60	182.5	133.0	576.2	710.2	2.06
Fe/Cr 50 : 50	182.5	133.1	576.5	710.7	2.13
Fe/Cr 60 : 40	182.5	133.1	576.6	710.9	2.09
Fe/Cr 70 : 30	182.4	133.1	576.6	710.8	2.46
Fe/Cr 80 : 20	182.4	133.1	576.4	710.3	2.19
Fe/Cr 90 : 10	182.5	133.0	576.3	710.4	2.13

Fe/Cr ratios versus nominal Fe/Cr ratio are plotted in Fig. 5. The resulting curves are almost coincident for Fe/Cr ratios ranging from 10/90 to 60/40, with very moderately higher affinity of the phosphate surface for Cr^{3+}. At higher Fe/Cr ratios, the phosphate surface shows a clear increasing preference for Cr^{3+}. This finding could suggest that the linkage of the mixed oligomers to the phosphate layer is taking place through Cr^{3+} ions. These data are also indicative of the absence of individual oxide precipitation.

XPS spectra of the pillared materials corresponding to the Cr $2p$ core level are shown in Fig. 6. The Cr $2p_{3/2}$ peak of samples 10/90 to 60/40 are asymmetric, due likely to multiplet splitting, but samples 70/30 to 90/10 clearly display a shoulder at higher binding energy (≈577.7 eV) which is characteristic of Cr(VI) (15). For the Fe-rich samples,

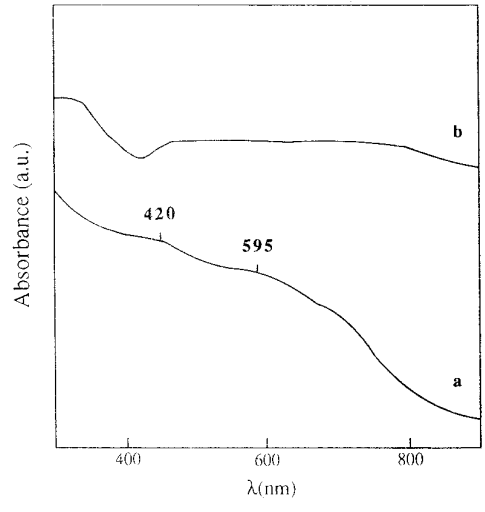

FIG. 7. Diffuse reflectance UV–VIS spectra of (a) intercalate with Fe/Cr 10/90 ratio and (b) pillared material Fe/Cr 10/90 at 400°C.

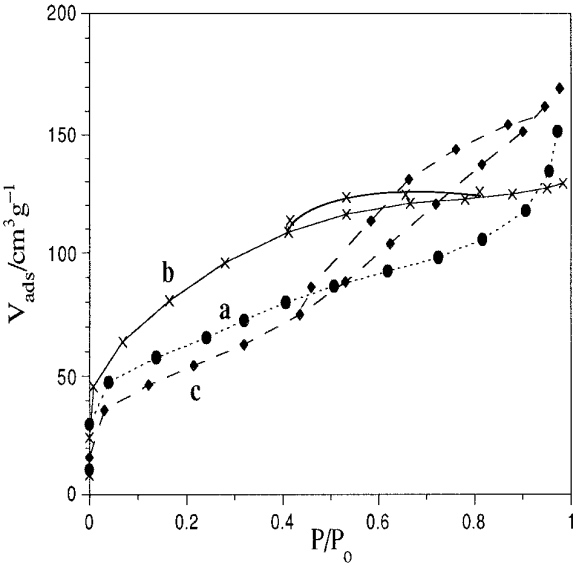

FIG. 8. Adsorption–desorption isotherms for Fe/Cr pillared materials at 400°C (under N_2): (a) 10/90, (b) 50/50 and (c) 90/10.

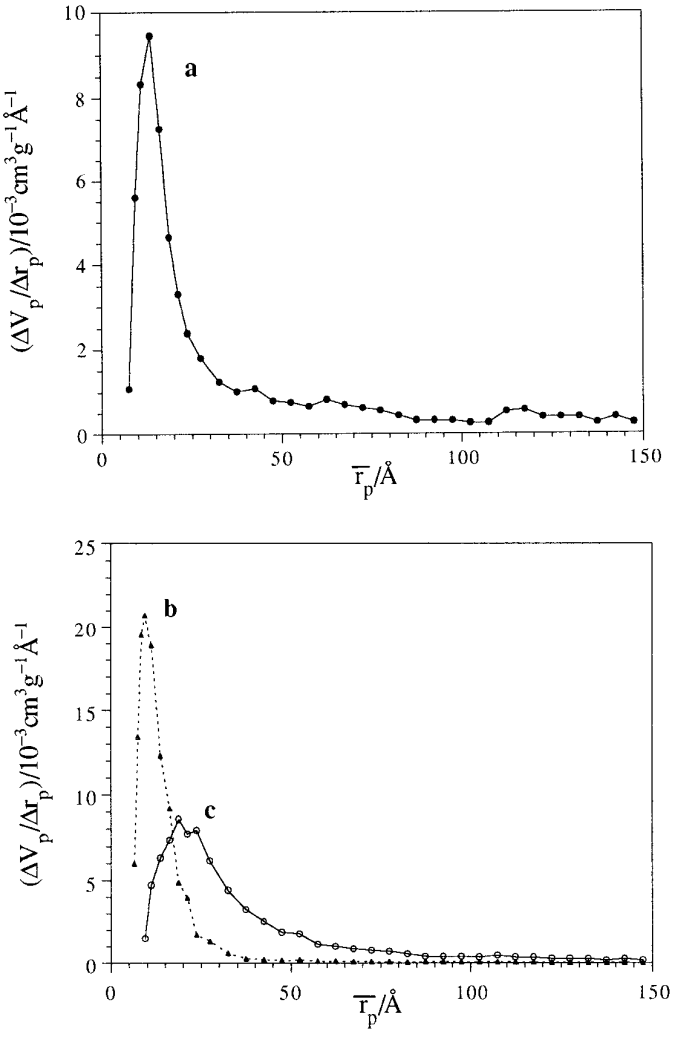

FIG. 9. Pore size distributions of Fe/Cr pillared materials: (a) 10/90, (b) 50/50, and (c) 90/10.

the surface Fe/Cr ratios deviate largely from those expected from bulk composition, suggesting that high dispersion of Cr(III) on the phosphate surface favors its oxidation to Cr(VI), in agreement with thermal analysis observations. Similar behavior was found in supported chromia catalysts (14). It can be noted that partial oxidation of Cr(III) in pillared materials takes place after calcination even in an inert atmosphere. The Mössbauer spectra of mixed Fe/Cr pillared materials indicate that the iron is in high spin 3+ state in all cases (16). The oxidation mechanism of Cr(III) is unclear and further studies are required for its elucidation.

BE values of the mixed Fe/Cr pillared materials are summarized in Table 3. P 2*p* and Zr $3d_{5/2}$ BE values are, in all cases, very similar to those found in α-ZrP (17), suggesting that the phosphate layer framework is preserved after pillaring with the mixed oxides. This is further confirmed by the P/Zr ratios found, which in most cases are very close to the theoretical ratio (P/Zr = 2). Slight changes in BE from 576.2 to 576.6 eV and from 711.1 to 710.2 eV are found for Cr $2p_{3/2}$ and Fe $2p_{3/2}$, respectively. Samples 40/60, 80/20, and 90/10 display the lowest values. The later samples exhibit the greatest differences in bulk and surface Fe/Cr compositions. The highest values of B.E. for Fe

TABLE 4
Textural Parameters for Mixed Fe/Cr Oxide Pillared α-Zirconium Phosphates and Mixed Oxide Powders

	S_{BET}(m^{2}g^{-1})	C_{BET}	V_{micro}(cm^3 g^{-1})[a]
Sample Fe/Cr			
10/90	216.0	262.1	0.10
20/80	241.2	161.0	0.10
30/70	200.0	110.0	0.08
40/60	261.6	116.3	0.10
50/50	305.9	117.7	0.13
60/40	212.8	100.1	0.08
70/30	285.8	113.7	0.11
80/20	195.7	105.8	0.08
90/10	189.2	126.5	0.09
Mixed oxides Fe/Cr			
10/90	275.9	41.8	0.14
50/50	142.8	409.1	0.06
90/10	111.7	165.1	0.04

[a] Calculated from the Dubinin equation.

$2p_{3/2}$ are found in the sample with lowest Fe/Cr ratios, indicating that when Fe^{+3} is incorporated in small amounts into the Cr_2O_3 network, the Fe 2*p* core levels of the Fe^{+3} ions are shifted to higher energies due to the more intense crystal field of this lattice.

The diffuse reflectance UV–VIS spectra of the samples are very complicated due to the overlapping of the absorption bands of Cr^{3+} and Fe^{3+}. The typical bands $^4T_{2g} \leftarrow {}^4A_{2g}$ and $^4T_{1g} \leftarrow {}^4A_{2g}$ of octahedral Cr^{3+} are masked with the transition metal-to-metal and ligand–metal charge transfers, in Fe^{3+}, which appear between 600 and 450 nm. The bands of octahedral Cr^{3+} at 420 and 595 nm (Fig. 7) appear only in the case of the intercalation compound with the lowest Fe^{3+} content (sample 10 : 90); in calcined materials only a continuous and strong absorption appears in this region of the spectrum.

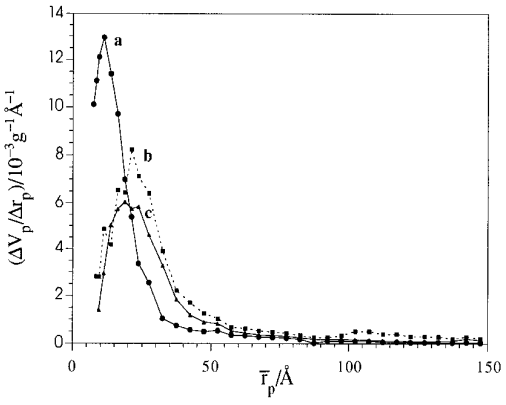

FIG. 10. Pore size distributions of Fe/Cr 20/80 pillared material calcined at 400°C: (a) under N_2, (b) in air, (c) sample (a) after further calcination in air.

Surface Area and Porosity

Figure 8 shows the adsorption–desorption isotherms of N_2 at 77 K for three representative pillared materials, prepared under N_2 at 400°C. According to the type of isotherm, two groups of materials can be distinguished. Group I corresponds to microporous solids (type I in BDDT classification) with some contribution of mesopores (18). Materials in this group have Fe/Cr ratios lower than 80/20 and BET surface areas higher than 200 m^2g^{-1}. Group II includes materials 80/20 and 90/10, with type IV isotherms, typical of mesoporous solids, but with a certain contribution of micropores. The BET surface areas for these materials are lower than 200 m^2g^{-1}. Table 4 lists the BET surface area and micropore volume data for all samples studied, including those of mixed oxides prepared from the precipitates. In all cases BET surface areas and micropore volumes are higher for the pillared materials. These textural parameters can be also compared with those reported for mixed Fe/Cr oxide powders, whose specific surface areas hardly reach to 100 $m^2\ g^{-1}$ (13). Interestingly, the oxide obtained from an acetate solution with an Fe/Cr ratio of 10/90 presents an unusually high S_{BET} of 276 $m^2\ g^{-1}$, as a consequence of the incorporation of a significant amount of acetate (associated to Cr^{3+}) into the precipitate, which decomposes upon calcination leaving a porous structure. This method may be used to prepare some highly porous mixed Fe/Cr oxides.

Pore size distributions, determined by the Cranston–Inkley method (19), are shown in Fig. 9. Samples of group I present a very narrow pore size distribution, between 7.5 and 15 Å, while for samples of group II the distribution is wider.

If the intercalates are directly calcined in air at 400°C or the pillared materials obtained under N_2 are exposed to further calcination in air at 400°C, the specific surface areas decrease and the pore size distribution is shifted toward larger pores (Fig. 10). These modifications may be explained as due to partial oxidation of Cr(III) to Cr(VI) with formation of CrO_3, which is subsequently segregated from the interlayer region (20). This would induce morphological changes in the particles in such a way that the mesoporosity is increased at the same time that the microporosity is decreased. These changes suggest an easy method to modify the porosity for specific purposes.

ACKNOWLEDGMENTS

This research was supported by the European Community, Program BRITE-EURAM, Contract BRE2-CT93-0450, and by the CICYT (Spain), Project MAT94-0678.

REFERENCES

1. C. A. C. Sequeira and M. J. Hudson, "Multifunctional Mesoporous Inorganic Solids," Kluwer, Dordrecht, 1993.
2. R. Burch, "*Catalysis Today, Pillared Clays.*" Elsevier, Amsterdam, 1988.
3. I. V. Mitchell, "Pillared Layered Structures: Current Trends and Applications." Elsevier, London, 1990.
4. P. Olivera-Pastor, J. Maza-Rodriguez, P. Maireles-Torres, E. Rodriguez-Castellon, and A. Jimenez-Lopez, *J. Mater. Chem.* **4,** 179 (1994).
5. D. Zhao, G. Wang, Y. Yang, X. Gou, Q. Wang, and J. Ren, *Clays Clay Miner.* **41** (3), 317 (1993).
6. L. Lloyd, D. E. Ridler, and M. V. Twigg, "*Catalyst Handbook*," 2nd ed. Wolfe, London, 1989.
7. E. H. Lee, *Catal. Rev.* **8,** 285 (1973).
8. H. H. Kung and M. C. Kung, *Adv. Catal.* **33,** 159 (1985).
9. H. Benhamza, A. Bouhaouss, F. A. Josien, and J. Livage, *J. Chim. Phys.* **88,** 1875 (1991).

10. C. F. Baes, Jr., and R. E. Mesmer, "*The Hydrolysis of Cations.*" Wiley, New York, 1978.
11. K. Nakamoto, "*The Infrared Spectra of Inorganic and Coordination Compounds*." Wiley-Interscience. New York, 1963.
12. A. Muan and S. Somiya, *J. Am. Ceram. Soc.* **43,** 201 (1960).
13. G. Busca, G. Ramis, M. C. Prieto, and V. Sánchez Escribano, *J. Mater. Chem.* **3** (6), 665 (1993).
14. S. E. Voltz and S. W. Welleer, *J. Am. Chem. Soc.* **76,** 4701 (1954).
15. O. S. Gorriz, U. Cortés, and J. L. G. Fierro, *Ind. En. Chem. Res.* **31,** 26 (1992).
16. F. J. Pérez-Reina, P. Olivera-Pastor, E. Rodríguez-Castellón, A. Jiménez-López, D. J. Jones, and J. Roziere, to be published.
17. E. Paparazzo, E. Severini, A. Jiménez-López, P. Maireles-Torres, P. Olivera-Pastor, E. Rodríguez-Castellón, and A. G. Tomlinson, *J. Mater. Chem.* **2** (11), 1175 (1992).
18. S. J. Gregg and K. S. W. Sing, "*Adsorption Surface Area and Porosity*," 2nd ed. Academic Press, Orlando, FL, 1982.
19. R. W. Cranston and F. A. Inkley, *Adv. Catal.* **9,** 143 (1957).
20. A. Jiménez-López, J. Maza-Rodríguez, P. Olivera-Pastor, P. Maireles-Torres, and E. Rodríguez-Castellón, *Clays Clay Miner.* **41**(3), 328 (1993).